J|A|C|S
ARTICLES
Published on Web 04/04/2002

[Ni^{0}L]-Catalyzed Cyclodimerization of 1,3-Butadiene: A Comprehensive Density Functional Investigation Based on the Generic [$(C_4H_6)_2Ni^0PH_3$] Catalyst

Sven Tobisch*,† and Tom Ziegler‡

Contribution from the Institut für Anorganische Chemie der Martin-Luther-Universität Halle-Wittenberg, Fachbereich Chemie, Kurt-Mothes-Strasse 2, D-06120 Halle, Germany, and Department of Chemistry, Universtity of Calgary, University Drive 2500, Calgary, Alberta, Canada T2N 1N4

Received October 15, 2001

Abstract: We present a comprehensive theoretical investigation of the mechanism for cyclodimerization of butadiene by the generic [bis(butadiene)Ni^{0}PH$_3$] catalyst employing a gradient-corrected DFT method. We have explored all critical elementary steps of the whole catalytic cycle, namely, oxidative coupling of two butadienes, reductive elimination under ring closure, and allylic isomerization. Oxidative coupling of two butadienes in the [bis(butadiene)Ni^{0}L] complex and reductive elimination in the [(bis(η^3)-octadienediyl)-Ni^{II}L] species take place under different stereocontrol, which makes isomerization indispensable. Commencing from a preestablished equilibrium between several configurations of the [(octadienediyl)Ni^{II}L] complex, the major cyclodimer products, namely, VCH, *cis*-1,2-DVCB, and *cis*,*cis*-COD, are formed along competing reaction paths via reductive elimination, which is found to be the overall rate-determining step. Careful exploration of different possible conceivable routes revealed that bis(η^1) species are not involved as critical intermediates either in reductive elimination or in isomerization along the most feasible pathway. The regulation of the selectivity of the cyclodimer formation based on both thermodynamic and kinetic considerations is outlined.

Introduction

The catalytic cyclodimerization of 1,3-dienes to give different cyclodimer products is an intriguing reaction and represents one of the famous textbook examples of a homogeneous catalytic reaction.[1] Several transition-metal complexes are known to actively catalyze the cyclodimerization reaction; however, nickel complexes represent the most versatile and useful catalytic systems.[2]

The first catalytic cyclodimerization of 1,3-butadiene to cycloocta-1,5-diene using modified Reppe catalysts was reported by Reed in 1954.[3] However, it remained for Wilke and co-workers to demonstrate the implications, versatility, and applicability of the nickel-catalyzed 1,3-diene cyclodimerization reactions.[2,4] The cyclodimerization of 1,3-dienes catalyzed by zerovalent ligand-stabilized nickel complexes is probably one of the mechanistically best investigated reactions in the whole of transition-metal catalysis, and it has played an important role in the development of homogeneous catalysis. Two fundamental catalytic principles were observed here for the first time: (I) that electronic and steric properties of a ligand correlate with a certain product composition, which nowadays is called "ligand tailoring", and (II) that the reactivity of this reaction is closely linked to its selectivity.

Without a catalyst, 1,3-butadiene can undergo thermal dimerization at elevated temperatures (270 °C), affording nearly exclusively 4-vinylcyclohexene (VCH).[5] This thermal [4 + 2] cycloaddition can formally be described as a Diels−Alder reaction between two butadienes in which one serves as the diene and the other as the dienophile (vinylethylene) component. Several mechanisms have been proposed for this process; the most popular are the concerted (symmetry-allowed) mechanism and the stepwise mechanism, which involves the formation of a bisallyl biradical intermediate. It has been shown in theoretical investigations that both mechanisms are similar in their energetics. Overall, thermal dimerization of butadiene has a barrier of ~29 kcal mol^{-1},[6] which requires severe reaction conditions.

* To whom correspondence should be addressed. E-mail: tobisch@chemie.uni-halle.de.
† University of Halle-Wittenberg.
‡ University of Calgary.

(1) (a) Jolly, P. W.; Wilke, G. The Oligomerization and Co-oligomerization of Butadiene and Substituted 1,3-Dienes. In *The Organic Chemistry of Nickel, Vol. 2, Organic Synthesis*; Academic Press: New York, 1975; pp 133-212. (b) Jolly, P. W. Nickel-Catalyzed Oligomerization of 1,3-Dienes Related Reactions. In *Comprehensive Organometallic Chemistry*; Wilkinson, G., Stone, F. G. A., Abel, E. W., Eds.; Pergamon: New York, 1982; Vol. 8, pp 671−711.
(2) (a) Wilke, G. *Angew. Chem., Int. Ed. Engl.* **1963**, *2*, 105. (b) Wilke, G. *Angew. Chem., Int. Ed. Engl.* **1988**, *27*, 185. (c) Wilke, G.; Eckerle, A. Cyclooligomerizations and Cyclo-Co-Oligomerizations of 1,3-Dienes. In *Applied Homogeneous Catalysis with Organometallic Complexes*; Cornils, B., Herrmann, W. A., Eds.; VCH: Weinheim, Germany, 1996; pp 358−373.
(3) Reed, H. W. B. *J. Chem. Soc.* **1954**, 1931.
(4) (a) Wilke, G. *Pure Appl. Chem.* **1978**, *50*, 677. (b) Wilke, G. *J. Organomet. Chem.* **1980**, *200*, 349.
(5) Ziegler, K.; Wilms, H. *Justus Liebigs Ann. Chem.* **1950**, *567*, 1.

Chart 1

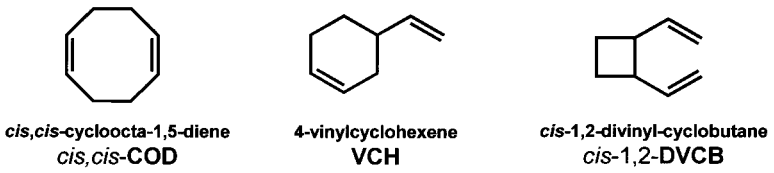

Chart 2

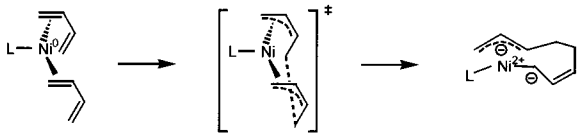

The mass of experimental evidence that has been generated indicates that the [Ni^0L]-catalyzed cyclodimerization of 1,3-dienes is the result of a multistep mechanism[2,7] and not due to a one-step concerted suprafacial fusion of two 1,3-diene moieties.[8] The nickel atom template undergoes a repeated change in its formal oxidation state; namely, [$Ni^0 \leftrightarrow Ni^{II}$], during the multistep addition−elimination mechanism. The zerovalent, "ligand-stabilized" [bis(butadiene)Ni^0L] complex is the active catalyst, where the ligand L typically is an alkyl-/arylphosphine PR_3 or phosphite $P(OR)_3$, respectively. The catalyst is conveniently prepared according to the general method established by Wilke et al. by reducing a nickel salt (commonly with an organoaluminum compound) in the presence of the ligand L and of butadiene.[9] Alternatively, a zerovalent nickel−ligand complex can be used instead, from which the catalyst is formed via organoligand displacement with butadiene.[2a] This catalyst cyclodimerizes butadiene at moderate conditions (80 °C) to a mixture of three major C_8 cyclohydrocarbons:[10] namely, *cis,cis*-cycloocta-1,5-diene (*cis,cis*-COD), *cis*-1,2-divinylcyclobutane (*cis*-1,2-DVCB), and 4-vinylcyclohexene (VCH) (cf. Chart 1). The composition of the cyclodimer products can be influenced by varying the reaction conditions and the ligand L. Of the three cyclodimers, *cis,cis*-COD is the only product that can be formed with a yield >95%.[11,12]

In contrast to the thermal dimerization of butadiene, in cyclodimerization catalyzed by late transition metals, the electron-rich metal M^0 acts as a nucleophile which undergoes oxidation to M^{2+} during the butadiene coupling process (cf. Chart 2). Therefore, a mechanism involving a bisallyl biradical intermediate is not operative. The role of the metal in this process is 2-fold. First, it provides $2e^-$ (which prevents the formation of a diradical intermediate), and second, it has the ability to polarize the butadiene, thus, allowing for different modes of the M^{2+}−bis(allyl−anion) coordination in the butadiene coupling product (cf. Chart 3). The stability and reactivity of the M^{2+}−bis(allyl−anion) coordination modes is essentially influenced by the donor strength and the steric bulk of the ligand L. In the bis(η^3-allyl) species **A**, the negative charge is delocalized around the allylic moieties, which is the favored situation from a energetic point of view. In the η^3,η^1 species **B** and **C**, the negative charge on one of the allylic groups has to be localized on either a single C^1 (**B**) or on C^3 (**C**) atom, which is energetically less favorable compared with **A**. The localization of the negative charge, however, can be supported by a donating ligand L. The bis(η^1-allyl) species **D** and **E** should be the energetically least likely coordination mode, since their formation requires the energetically unfavored localization of the negative charge in both allylic moieties on a single carbon atom.

The M^{2+}−bis(allyl−anion) species **A**−**E** can undergo subsequent reductive elimination under C−C bond formation between the carbanionic centers affording the three principal cyclodimers (cf. Chart 3). The subtle energetic balance between the oxidative coupling and the reductive elimination steps, which is influenced by the redox properties ($M^0 \leftrightarrow M^{2+}$) of the metal, is of fundamental importance for a facile transition-metal-mediated cyclodimerization of 1,3-dienes.

The general catalytic cycle for the [Ni^0L]-catalyzed cyclodimerization of butadiene is shown in Scheme 1 which in the essential parts is based on the mechanistic proposal of Wilke et al..[2,13] However, it contains additional conceivable reaction routes for cyclodimer formation and addresses the role of allylic isomerization. Commencing from the [bis(butadiene)Ni^0L] active catalyst **1**, the two coordinated butadiene moieties undergo oxidative coupling resulting in the formation of the [(octadienediyl)$Ni^{II}L$] complex. This [(octadienediyl)$Ni^{II}L$] complex represents the crucial species of the catalytic cycle and has been demonstrated to exist in several configurations. These configurations can be classified according to the different coordination of the two terminal allylic groups, namely, the η^3,η^1 species **2** and **3**; the bis(η^3) species **4**; and the bis(η^1) species **5**, **6**, and **7**. All of these species are in equilibrium, and their relative abundance has been shown to be strongly dependent on the electronic and steric properties of the ligand L. The cyclodimer products are formed along three reaction paths via reductive elimination under ring closure starting from different [(octadienediyl)$Ni^{II}L$] species. The products are the [(cyclodimer)Ni^0L] complexes **8**, **9**, and **10**, respectively, which may be stabilized by coordination of an additional butadiene. Expulsion of the cyclodimers in a subsequent substitution with butadiene, which is supposed to take place without a significant barrier, regenerates the active catalyst **1**, thus completing the catalytic cycle. VCH is formed along the reaction path starting from the [(η^3,η^1-(C^1)-octadienediyl)$Ni^{II}L$] species **2**, while the [(bis(η^3)-octadienediyl)$Ni^{II}L$] species **4** acts as precursor for the generation of

(6) (a) Vaughan, W. E. *J. Am. Chem. Soc.* **1932**, *54*, 3863. (b) Kistiakowski, G. B.; Ransom, W. W. *J. Chem. Phys.* **1939**, *7*, 725. (c) Huybrechts, G.; Luyckx, L.; Vandenboom, T.; van Mele, B. *Int. J. Chem. Kinet.* **1977**, *9*, 283.
(7) Heimbach, P.; Jolly, P. W.; Wilke, G. *Adv. Organomet. Chem.* **1970**, *8*, 29.
(8) (a) Mango, F. D. *Adv. Catal.* **1969**, *20*, 291 (b) Mango, F. D. *Tetrahedron Lett.* **1969**, 4813.
(9) Wilke, G.; Müller, E. W.; Kröner, M.; Heimbach, P.; Breil, H. DBP 1191375 (Prior. 28. 4), 1960.
(10) A fourth cyclodimer of butadiene, the 1-methylene-2-vinylcyclopentane (MVCP), is formed in the presence of secondary alcohols. This reaction, however, is not investigated in the present study.
(11) Brenner, W.; Heimbach, P.; Hey, H.; Müller, E. W.; Wilke, G. *Justus Liebigs Ann. Chem.* **1967**, *727*, 161.
(12) (a) Heimbach, P.; Kluth, J.; Schenkluhn, H.; Weimann, B. *Angew. Chem., Int. Ed. Engl.* **1980**, *19*, 569. (b) Heimbach, P.; Kluth, J.; Schenkluhn, H.; Weimann, B. *Angew. Chem., Int. Ed. Engl.* **1980**, *19*, 570.
(13) Benn, R.; Büssemeier, B.; Holle, S.; Jolly, P. W.; Mynott, R.; Tkatchenko, I.; Wilke, G. *J. Organomet. Chem.* **1985**, *279*, 63.

Chart 3

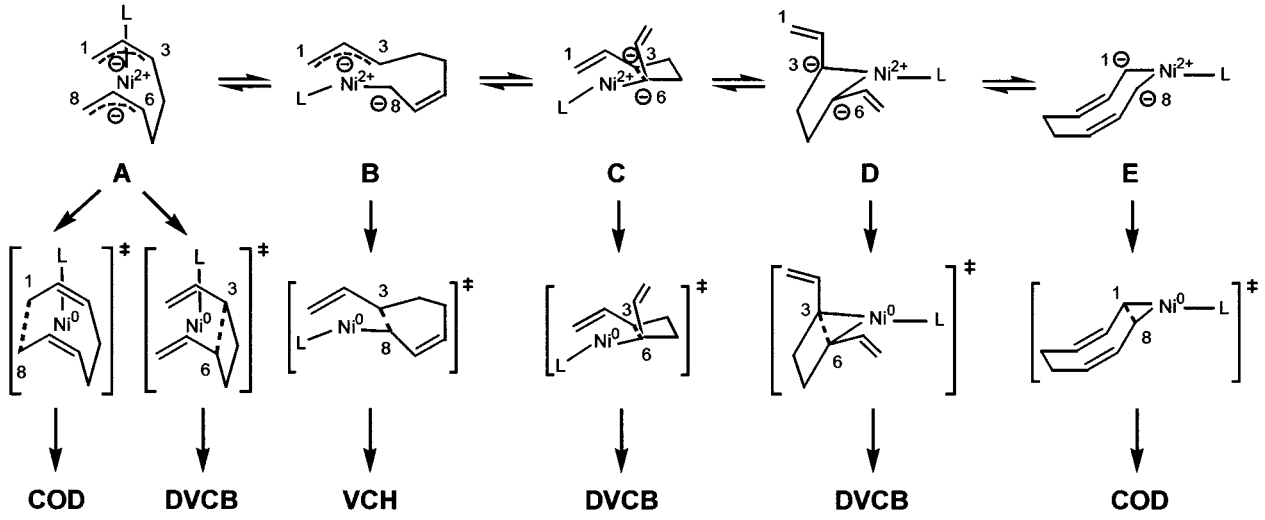

Scheme 1. Catalytic Cycle of the [Ni⁰L]-Catalyzed Cyclodimerization of Butadiene

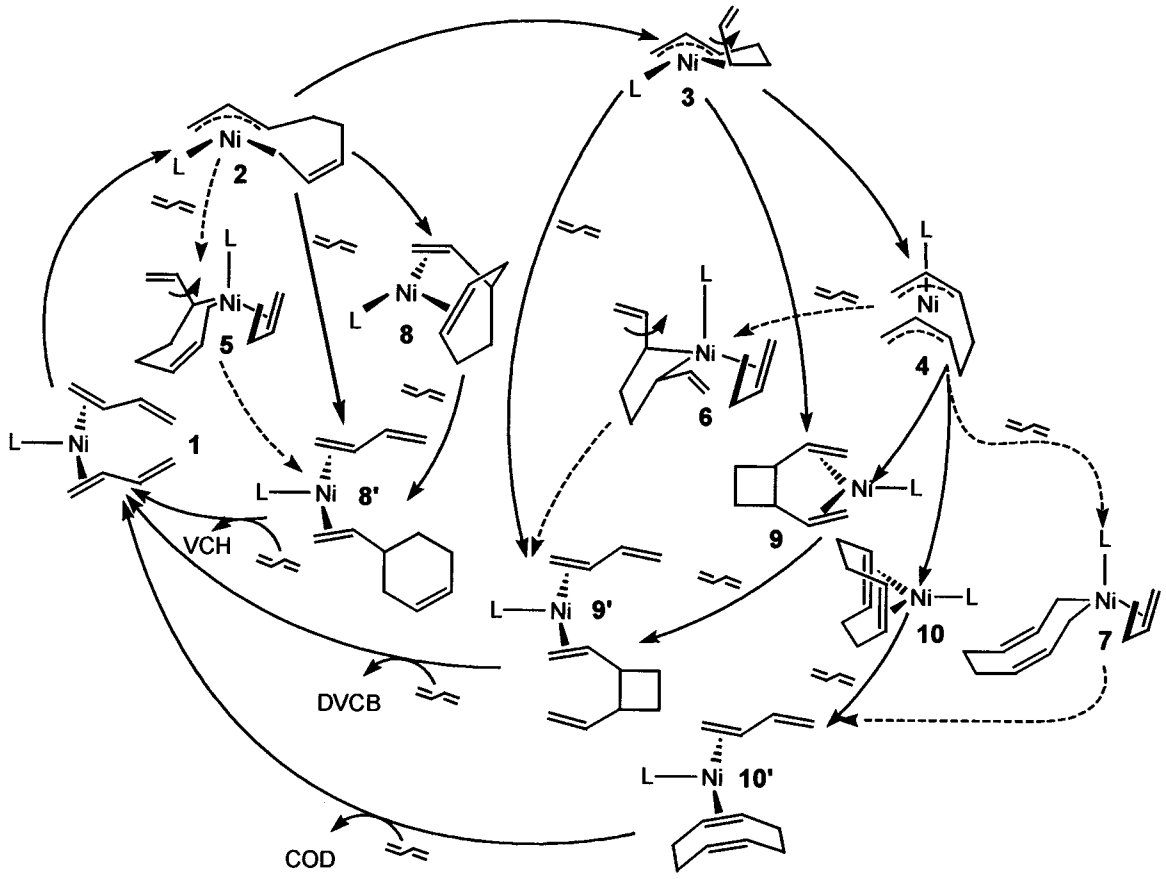

DVCB and COD, respectively. An alternative route, however, is conceivable for the formation of DVCB, which starts from the [(η^3,η^1(C^3)-octadienediyl)Ni^{II}L] species **3**. The isomerization of the terminal allylic groups of the [(octadienediyl)Ni^{II}L] complex represents a further critical elementary reaction step. A substrate-specific termination reaction, however, has never been observed.

Two different mechanistic proposals have emerged for the reductive elimination under ring closure. They differ in the suggested coordination mode of the allylic groups in the species that are involved as key intermediates. In the first mechanism,[14] the reductive elimination is believed to take place directly starting from the [(η^3-π-octadienediyl)Ni^{II}L] species (indicated by solid lines for all reductive elimination processes in Scheme 1), i.e., along the **2** → **8** route as exemplified for the formation of VCH. In the second mechanism,[4,13] [(bis(η^1-σ)-octadienediyl)-Ni^{II}L] species are suggested as key intermediates (indicated by dashed lines for the reductive elimination processes in Scheme 1), which means that f.i. VCH should be generated following the **2** → **5** → **8** route. The structure of the [(octadienediyl)-

(14) Heimbach, P.; Traunmüller, R. *Chemie der Metall-Olefin-Komplexe*; Verlag Chemie GmbH: Weinheim, 1970.

$Ni^{II}L$] species **2** and **4** has been unequivocally established both by NMR and by X-ray structural analysis.[13,15] The intermediacy of the [(bis(η^1)-octadienediyl)$Ni^{II}L$] species **5**, **6**, and **7**, however, is highly speculative since they have never been experimentally characterized.

The proposed catalytic cycle in Scheme 1 has been decisively supported by the stoichiometric cyclodimerization reaction.[13] For butadiene as well as substituted 1,3-dienes **2** (η^3-syn,η^1-(C^1),Δ-cis isomer) and **4** (bis(η^3-syn) isomer) has been firmly established as key reaction intermediates,[13,15] thus, eliminating a single-step concerted reaction as a possibility. Further evidence in favor of a multistep mechanism comes from the determination of the stereochemistry of cyclodimer products that are formed from substituted 1,3-dienes[16] as well as from deuterium-labeled butadienes.[17] It has been shown that zerovalent nickel−ligand complexes react with butadiene to yield initially **2**, which undergoes rearrangement to **4** from which [(COD)Ni^0L] is formed by reductive elimination.[7,13] The species **2** has been identified as the precursor for the reductive elimination path that affords VCH, and indirect evidence has been provided for **4** acting as precursor for the formation of DVCB.[13] The reversibility of both the reductive elimination and the oxidative coupling has been demonstrated.[13,15a,18]

There is no doubt that the fundamental, systematic, and comprehensive work of Wilke et al. has led to a thorough understanding of how the [Ni^0L]-catalyzed cyclodimerization of butadiene does operate. There are, however, some mechanistic details that are not yet firmly established. (I) Which of the two mechanistic proposals is operative for the reductive elimination step? (II) What is the geometric structure of the active [bis-(butadiene)Ni^0L] catalyst complex? (III) How does oxidative coupling of two coordinated butadiene moieties in **1** most likely proceed? *(IV)* What is the role of the isomerization of the terminal allylic groups of the [(octadienediyl)$Ni^{II}L$] complex in the catalytic cycle? (V) Which of the crucial elementary reaction processes is rate-determining?

The present theoretical study is aimed at improving the mechanistic insight into the [Ni^0L]-catalyzed cyclodimerization of butadiene by clarifying these intriguing questions. The entire catalytic cycle is explored by means of quantum chemical calculations that employ a gradient-corrected density functional method. All critical elementary reactions proceeding along different conceivable routes have been scrutinized, taking into account oxidative coupling, reductive elimination under ring closure, and allylic isomerization. The present study is to the best of our knowledge the first theoretical mechanistic investigation aiming at the exploration and elucidation of the complete catalytic cycle for the [Ni^0L]-catalyzed cyclodimerization of butadiene.[19]

In the current study, we explore the catalytic cycle for a generic [bis(butadiene)Ni^0PH_3] catalyst. The regulation of the selectivity in the cyclodimer formation depending on the electronic and steric properties of the ligand L, however, is examined in a subsequent paper.

Computational Details

All reported DFT calculations were performed by using the TURBOMOLE program package developed by Häser and Ahlrichs.[20] The local exchange-correlation potential by Slater[21a,b] and Vosko et al.[21c] was augmented with gradient-corrected functionals for electron exchange according to Becke[21d] and correlation according to Perdew[21e] in a self-consistent fashion. This gradient-corrected density functional is usually termed BP86 in the literature. In recent benchmark computational studies, it was shown that the BP86 functional gives results in excellent agreement with the best wave function-based method available today, for the class of reactions investigated here.[22]

For all atoms, a standard all-electron basis set of triple-ζ quality for the valence electrons augmented with polarization functions was employed for the geometry optimization and the saddle-point search. The Wachters 14s/9p/5d set[23a] supplemented by two diffuse p[23a] and one diffuse d function[23b] contracted to (62111111/5111111/3111) was used for nickel, and standard TZVP basis sets[23c] were used for phosphorus (a 13s/9p/1d set contracted to (73111/6111/1)), for carbon (a 10s/6p/1d set contracted to (7111/411/1)), and for hydrogen (a 5s/1p set contracted to (311/1)). The frequency calculations were done by using standard DZVP basis sets,[23c] which consist of a 15s/9p/5d set contracted to (63321/531/41) for nickel, a 12s/8p/1d set contracted to (6321/521/1) for phosphorus, a 9s/5p/1d set contracted to (621/41/1) for carbon, and a 5s set contracted to (41) for hydrogen. The corresponding auxiliary basis sets were used for fitting the charge density.[23c,d] This is the standard computational methodology utilized throughout this paper.

The geometry optimization and the saddle-point search were carried out by utilizing analytical/numerical gradients/Hessians according to standard algorithms. No symmetry constraints were imposed in any case. The stationary points were identified exactly by the curvature of the potential-energy surface at these points corresponding to the eigenvalues of the Hessian. The reaction and activation enthalpies and free energies (ΔH, ΔG and $\Delta H^{\ddagger}$, $\Delta G^{\ddagger}$ at 298 *K* and 1 atm) were calculated for the most stable isomers of each of the key species of the entire catalytic reaction. The pictorial representation of key species involved in the important elementary steps along the most feasible pathways are available as Supporting Information (Figures S1−S6).

Results and Discussion

We shall start our investigation by exploring each of the elementary processes in Scheme 1 for the generic [bis-(butadiene)Ni^0PH_3] catalyst. We shall further discuss how thermodynamic and kinetic factors regulate the selectivity of the cyclodimer production.

A. Oxidative Coupling of Two Coordinated Butadienes. Depending on the mode of butadiene coordination, different

(15) (a) Jolly, P. W.; Tkatchenko, I.; Wilke, G. *Angew. Chem., Int. Ed. Engl.* **1971**, *10*, 329. (b) Brown, J. M.; Golding, B. T.; Smith, M. J. *Chem. Commun.* **1971**, 1240. (c) Barnett, B.; Büssemeier, B.; Heimbach, P.; Jolly, P. W.; Krüger, C.; Tkatchenko, I.; Wilke, G. *Tetrahedron Lett.* **1972**, 1457. (d) Büssemeier, B. Doctoral Thesis, University of Bochum, 1973. (e) Jolly, P. W.; Mynott, R.; Salz, R. *J. Organomet. Chem.* **1980**, *184*, C49.

(16) (a) Heimbach, P.; Hey, H. *Angew. Chem., Int. Ed. Engl.* **1970**, *9*, 528. (b) Buchholz, H.; Heimbach, P.; Hey, H.-J.; Selbeck, H.; Wiese, W. *Coord. Chem. Rev.* **1972**, *8*, 129. (c) Heimbach, P. *Angew. Chem., Int. Ed. Engl.* **1973**, *12*, 975.

(17) (a) Yamamoto, A.; Morifuji, K.; Ikeda, S.; Saito, T.; Uchida, Y.; Misono, A. *J. Am. Chem. Soc.* **1968**, *90*, 1878. (b) Graham, C. R.; Stephenson, L. M. *J. Am. Chem. Soc.* **1977**, *99*, 7098.

(18) Heimbach, P.; Brenner, W. *Angew. Chem., Int. Ed. Engl.* **1967**, *6*, 800.

(19) There is one molecular mechanics study of limited predicting power that is restricted to only one subject of the whole mechanism: Gugelchuk, M. M.; Houk, K. N. *J. Am. Chem. Soc.* **1994**, *116*, 330.

(20) (a) Häser, M.; Ahlrichs, R. *J. Comput. Chem.* **1989**, *10*, 104. (b) Ahlrichs, R.; Bär, M.; Häser, M.; Horn, H.; Kölmel, C. *Chem. Phys. Lett.* **1989**, *62*, 165.

(21) (a) Dirac, P. A. M. *Proc. Cambridge Philos. Soc.* **1930**, *26*, 376. (b) Slater, J. C. *Phys. Rev.* **1951**, *81*, 385. (c) Vosko, S. H.; Wilk, L.; Nussiar, M. *Can. J. Phys.* **1980**, *58*, 1200. (d) Becke, A. D. *Phys. Rev.* **1988**, *A38*, 3098. (e) Perdew, J. P. *Phys. Rev.* **1986**, *B33*, 8822.; *Phys. Rev. B* **1986**, *34*, 7406.

(22) (a) Bernardi, F.; Bottoni, A.; Calcinari, M.; Rossi, I.; Robb, M. A. *J. Phys. Chem.* **1997**, *101*, 6310. (b) Jensen, V. R.; Børve, K. *J. Comput. Chem.* **1998**, *19*, 947.

(23) (a) Wachters, A. H. J. *J. Chem. Phys.* **1970**, *52*, 1033. (b) Hay, P. J. *J. Chem. Phys.* **1977**, *66*, 4377. (c) Godbout, N.; Salahub, D. R.; Andzelm, J.; Wimmer, E. *Can. J. Chem.* **1992**, *70*, 560. (d) TURBOMOLE basis set library.

Table 1. Thermodynamic Stability ($\Delta H/\Delta G$ in kcal mol^{-1}) of Different Forms of the Generic [Bis(butadiene)Ni^{0}PH$_3$] Catalyst Complex **1**[a,b]

η^4-t/η^2-t	η^4-t/η^2-c	η^4-c/η^2-t	η^4-c/η^2-c	η^2-t/η^2-t	η^2-c/η^2-t	η^2-c/η^2-c
8.3/*10.0*	12.1/*13.9*	4.7/*6.5*	6.7/*8.5*	0.0/*0.0*	3.0/*2.7*	4.6/*4.8*

[a] Only the most stable isomers for identical (*cis*/*cis*- or *trans*/*trans*-) or mixed *cis*/*trans*-butadiene coordination in η^4,η^2-butadiene and bis-η^2-butadiene forms of **1** are reported. [b] Numbers in italics are the Gibbs free energies.

forms are conceivable for the [bis(butadiene)Ni^{0}L] active catalyst complex **1**, all of which are in equilibrium. These are formal 16e$^-$ species with two η^2-butadienes, formal 18e$^-$ species with a mixed η^2,η^4-butadiene coordination, and formal 20e$^-$ species that arise from two η^4-coordinated butadienes. In all these species, each of the two butadienes can coordinate in either a cis or trans configuration. Furthermore, the prochiral butadiene can coordinate with one of its two different enantiofaces.

Several isomers of the trigonal planar bis(η^2-butadiene) form and the quasi tetrahedral η^4,η^2-butadiene form of **1** have been located on the potential energy surface as minimum points. Formal 20e$^-$ bis-η^4-butadiene species of **1**, however, could not be located. Starting from different initial structures, the 20e$^-$ species always relaxed into either bis(η^2-butadiene) or η^4,η^2-butadiene forms of **1**. The thermodynamic stability of the most favorable isomers for each of the bis(η^2)- and η^4,η^2-butadiene forms is collected in Table 1. For butadiene to coordinate in a bidentate fashion, the η^4-cis mode is energetically preferred relative to the η^4-trans mode, while the η^2-trans mode prevails for monodentate coordination.

Overall, the 16e$^-$ trigonal planar [bis(η^2-butadiene)Ni^{0}PH$_3$] species represents the most stable form of the active catalyst complex **1**, with the most stable isomer arising from a bis(η^2-trans) butadiene coordination. Although a [bis(butadiene)Ni^{0}L] complex has never been unambiguously characterized by experiment,[24a] formal 16e$^-$ trigonal planar [bis(olefin)Ni^{0}L] complexes are well known.[24b−e] Due to the higher flexibility of a η^2-butadiene, the energetic gap between 16e$^-$ and 18e$^-$ species is, as expected, enhanced by taking entropy contribution into account (ΔG). The order of the calculated stability for bis-(η^2-butadiene) isomers reflects the preference for the η^2-trans relative to the η^2-cis coordination. On the other hand, isomers arising from butadiene coordinating with different enantiofaces are close in energy.

The oxidative coupling was examined for both the bis(η^2-butadiene) and η^4,η^2-butadiene forms of **1**. In all cases, the formation of the new C−C σ-bond was found to take place via coupling of the outermost carbons of two η^2-butadienes (i.e., the terminal carbons of the noncoordinated olefinic subunit). Starting from the η^4,η^2-butadiene isomers of **1**, the systems always approach the corresponding bis(η^2-butadiene) species in the vicinity of the transition state. Thus, the route with bis-(η^2-butadiene) transition states is energetically preferred for all isomers of **1**. The coupling of the innermost carbons of two η^2-butadienes (i.e., the terminal carbons of the coordinated olefinic subunit), however, is found to be essentially repulsive in the initial stages and is therefore expected to be accompanied by a very high barrier. This observation agrees with findings from a computational study of the Ni^0-catalyzed ethylene dimerization.[25]

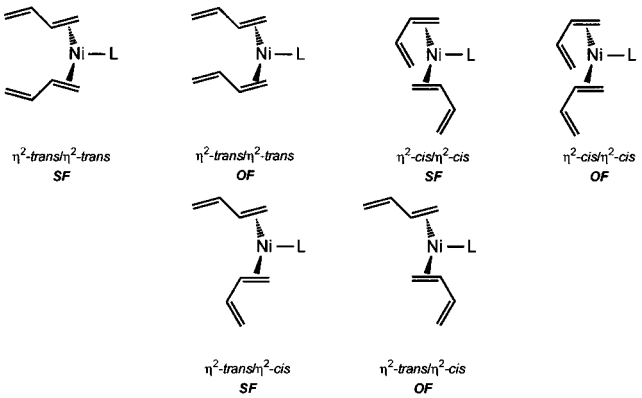

Figure 1. Different configurations and enantiofaces of the two butadienes in the [bis(η^2-butadiene)Ni^{0}L] catalyst complex **1** capable of undergoing oxidative coupling. SF and OF denotes the coordination of the two butadienes with either the same or the opposite enantioface, respectively.

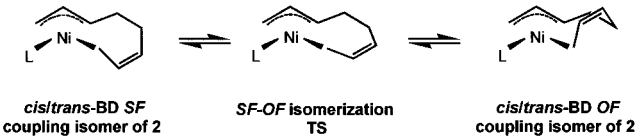

Figure 2. Conversion of the SF and OF butadiene coupling stereoisomers via SF−OF isomerization in **2**.

The enantiofaces of the two butadienes involved in the oxidative coupling play a crucial role for the stereocontrol of the cyclodimer formation. The two butadienes can couple either with the same enantioface (denoted SF; i.e., same face) or the opposite enantioface (denoted OF; i.e., opposite face), as exemplified in Figure 1 for the [bis(η^2-butadiene)Ni^{0}L] form of **1**. To rationalize the stereoselective cyclodimer formation we shall analyze the oxidative coupling step, the reductive elimination steps, and the interconversion of the anti and syn configuration of the terminal allylic groups in the [(octadiene-diyl)Ni^{II}L] complex with regard to the different stereoisomers involved. The transformation of the SF and OF butadiene coupling stereoisomers, which preferably proceeds in **2**, is discussed in section C2 (cf. Figure 2).

The energetics of the oxidative coupling along the different stereochemical pathways is collected in Table 2, and the key species involved are given in Figure S1 for two representative cases. The oxidative coupling of two butadienes in **1** occurs via formation of a new C−C σ-bond between the outermost carbons (C^4, C^5) of two η^2-butadienes, that happens at a distance of ∼2.0−2.2 Å in the transition states. The [(η^3,η^1(C^1)-octadienediyl)Ni^{II}PH$_3$] species **2** is formed as the kinetic product in an overall thermoneutral reaction, except for the coupling of two *trans*-butadienes which yields strained products. Both aspects are proven theoretically by following the reaction pathway going downhill from slightly relaxed transition-state structures.

(24) (a) Jolly, P. W.; Tkatchenko, I.; Wilke, G. *Angew. Chem., Int. Ed. Engl.* **1971**, *10*, 328. (b) Tolman, C. A.; Riggs, W. M.; Linn, W. J.; King, C. M.; Wendt, R. C. *Inorg. Chem.* **1973**, *12*, 2, 2770. (c) Giannoccaro, P.; Sacco, A.; Vasapollo, G. *Inorg. Chem. Acta* **1979**, *37*, L455. (d) Dreissig, W.; Dietrich, H. *Acta Crystallogr., Sect. B* **1981**, *37*, 931. (e) Pörschke, K.-R.; Wilke, G.; Mynott, R. *Chem. Ber.* **1985**, *118*, 298.

(25) Bernardi, F.; Bottoni, A.; Rossi, I. *J. Am. Chem. Soc.* **1998**, *120*, 7770.

Table 2. Activation Enthalpies and Free Energies ($\Delta H^{\ddagger}/\Delta G^{\ddagger}$ in kcal mol^{-1}) and Reaction Enthalpies and Free Energies ($\Delta H/\Delta G$ in kcal mol^{-1}) for Oxidative Coupling for the Generic [Bis(η^2-butadiene)Ni^{0}PH$_3$] Complex[a-c]

BD coupling[a]	*t*/*t*-BD SF	*t*/*t*-BD OF	*c*/*t*-BD SF	*c*/*t*-BD OF	*c*/*c*-BD SF	*c*/*c*-BD OF
1	0.0/*0.0*	0.4/*0.6*	3.0/*2.7*	3.9/*3.7*	4.6/*4.8*	5.0/*5.3*
TS[**1**−**2**]	12.0/*14.4*	15.0/*17.0*	20.9/*22.5*	**10.9/*13.6***	20.8/*22.3*	24.7/*26.8*
2	9.9/*12.1*	14.4/*16.6*	−0.1/*2.8*	−2.8/*0.1*	−2.0/*0.9*	2.7/*5.8*

[a] This process is classified according to the kind of butadiene coupling involved. [b] Absolute barriers and reaction energies relative to the most stable isomer of **1**, namely, [bis(η^2-*trans*-butadiene)Ni^{0}PH$_3$]. [c] Numbers in italics are the Gibbs free energies. [d] The lowest barrier of the individual stereochemical pathways is in boldface type.

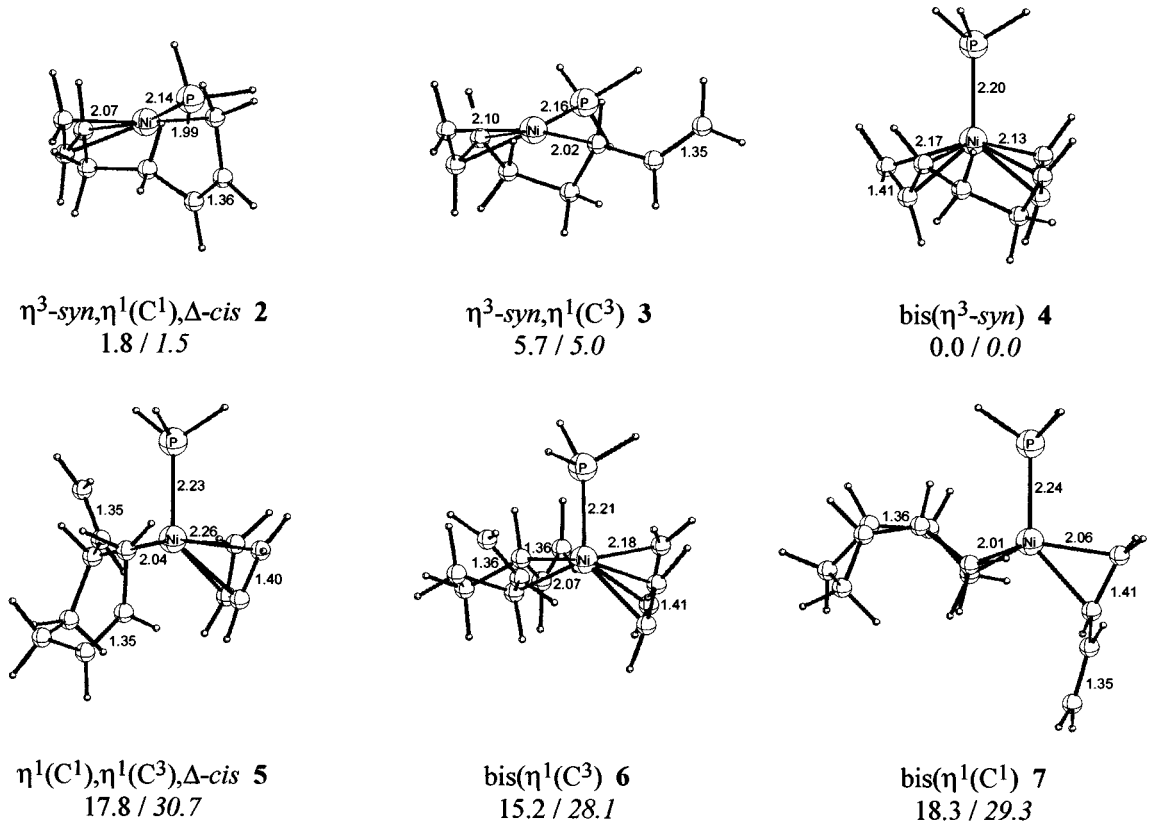

η^3-*syn*,η^1(C^1),Δ-*cis* **2**
1.8 / *1.5*

η^3-*syn*,η^1(C^3) **3**
5.7 / *5.0*

bis(η^3-*syn*) **4**
0.0 / *0.0*

η^1(C^1),η^1(C^3),Δ-*cis* **5**
17.8 / *30.7*

bis(η^1(C^3) **6**
15.2 / *28.1*

bis(η^1(C^1) **7**
18.3 / *29.3*

Figure 3. Most stable isomer for each of the different configurations **2**−**7** of the [(octadienediyl)Ni^{II}PH$_3$] complex, together with relative enthalpies (ΔH) and free energies (ΔG in italics).

For oxidative coupling to occur along the most feasible pathway, (η^2-cis/*trans*-butadiene OF) a free-energy barrier of 13.6 kcal mol^{-1} ($\Delta G^{\ddagger}$) has to be overcome. This pathway is also thermodynamically preferred by formation of the most stable isomer of the product species **2**. Our calculated geometry for this [(η^3-syn,η^1(C^1),Δ-cis,-octadienediyl)Ni^{II}PH$_3$] isomer of **2** closely parallels that of the experimentally isolated initial coupling product, which has been firmly established both by NMR[13] and X-ray.[15b] A slightly higher free-energy barrier of 14.4 kcal mol^{-1} ($\Delta G^{\ddagger}$) arises from the SF coupling of two *trans*-butadienes, which, however, gives rise to a highly strained product. The coupling of two *cis*-butadienes, on the other hand, is precluded by a prohibitively high barrier of 22.3 kcal mol^{-1} ($\Delta G^{\ddagger}$ for SF coupling) that arises from the unfavored rotation of both butadiene moieties from a energetically preferred inplane orientation in **1** to a nearly upright (perpendicular to the trigonal planar coordination plane) orientation in the transition states.

B. Thermodynamic Stability of Different [(octadienediyl)-Ni^{II}L] Species. The [(octadienediyl)Ni^{II}L] complex is the key species for the mechanistic cycle in Scheme 1. The different species **2**−**7** represent either precursors or proposed intermediates for the final reductive elimination processes or act as precursors for isomerization of the terminal allylic groups. All the species **2**−**7** are supposed to be in a dynamic equilibrium, since there is no experimental evidence for a significant kinetic barrier associated with the interconversion of the different [(octadienediyl)Ni^{II}L] species.

There are several isomers for each species **2**−**7**, most of which have been examined. Since we focus here on the relative thermodynamic stability of the different [(octadienediyl)Ni^{II}-PH$_3$] species, only the most stable isomer for each species **2**−**7** are discussed. They are displayed together with their relative energies in Figure 3. The square-planar η^3,η^1(C^1) species **2** and the square-pyramidal bis(η^3-syn) species **4** are the most stable isomers of the [(octadienediyl)Ni^{II}PH$_3$] complex. For the generic PH$_3$ ligand **4** is thermodynamically slightly preferred over **2** by 1.5 kcal mol^{-1} (ΔG). Concerning the two η^3,η^1 isomers **2** and **3**, the η^3,η^1(C^1) species **2** is calculated to be energetically more favorable by 3.5 kcal mol^{-1} (ΔG) relative to the η^3,η^1(C^3) species **3**. For the bis(η^1) species we found the coordination of an additional butadiene necessary for coordinative stabilization. Overall, the bis(η^1) species **5**−**7** represents energetically high

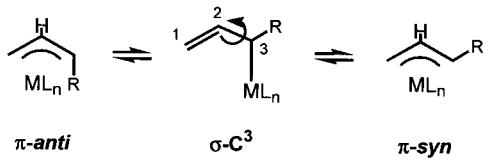

Figure 4. Isomerization of an η^3-π-allylic group taking place via an η^1-σ-C^3-allylic intermediate.

lying isomers of the [(octadienediyl)Ni^{II}PH$_3$] complex, which are energetically well separated by at least 10 kcal mol^{-1} (ΔH) from the η^3-octadienediyl species **2**−**4**. The energetic gap between the η^3 and bis(η^1) species is increased by another 11−13 kcal mol^{-1} at the free-energy surface (ΔG) as a result of the decrease in entropy associated with butadiene coordination.

Of the different species for the [(octadienediyl)Ni^{II}PH$_3$] complex found in equilibrium, **2** and **4** are seen from Figure 3 to be the prevalent species with similar populations whereas the concentration for **5**−**7** will be negligible.

C1. Syn−Anti Isomerization of the Terminal Allylic Groups in the [(Octadienediyl)Ni^{II}L] Complex. The interconversion of the anti and syn configuration of the terminal allylic groups in the [(octadienediyl)Ni^{II}L] complex represents a crucial elementary step for the following reasons: (I) The bis(η^3-syn) isomer of **4** has been unequivocally observed by tracing the stoichiometric cyclodimerization by NMR.[13] Instead of the corresponding stereoisomer of COD, namely, *trans*,*trans*-COD, however, the *cis*,*cis*-COD is formed, which makes isomerization indispensable. (II) On the other hand, the precursor for affording *cis*,*cis*-COD, namely, the bis(η^3-anti) isomer of **4**, is less likely to be formed along a reaction route without isomerization steps involved due to the prohibitively high barrier for coupling of two *cis*-butadienes (section A). This let us to conclude that an isomerization step is likely to be involved along the reaction path that affords *cis*,*cis*-COD. (III) The kinetic barriers for individual stereochemical pathways for oxidative coupling and reductive elimination affording DVCB and COD calculated in the present study (section A, D2 and D3) reveal that these steps operate under different stereocontrol since opposite stereoisomers are involved along the most feasible pathway for each of the steps.

It has not been possible by NMR to measure rates of isomerization in stoichiometric cyclodimerization, even at much lower temperatures (−30 to 25 °C) than those used in catalytic cyclodimerization (80 °C). This may indicate that isomerization is too fast to be observed at the NMR time scale.

The interconversion of the two isomeric forms of the η^3-butenyl−transition-metal bond, namely, η^3-anti and η^3-syn, most likely takes place by means of a η^3-$\pi \rightarrow \eta^1$-σ-C^3 allylic group conversion, followed by internal rotation of the vinyl group around the C^2−C^3 single bond (cf. Figure 4). This has been confirmed both by experimental[26] and by theoretical[27] evidence. As a result of isomerization, the configuration on C^3 (anti → syn, or vice versa) is changed and gives rise to an inversion of chirality on C^2.[26b]

(26) (a) Faller, J. W.; Thomsen, M. E.; Mattina, M. J. *J. Am. Chem. Soc.* **1971**, *93*, 2642. (b) Lukas, J.; van Leeuwen, P. W. N. M.; Volger, H. C.; Kouwenhoven, A. P. *J. Organomet. Chem.* **1973**, *47*, 153. (c) Vrieze, K. Fluxional Allyl Complexes. In *Dynamic Nuclear Magnetic Resonance Spectroscopy*: Jackman, L. M., Cotton, F. A., Eds.; Academic Press: New York, 1975.

(27) Tobisch, S.; Taube, R. *Organometallics* **1999**, *18*, 3045.

Table 3. Activation Enthalpies and Free Energies ($\Delta H^{\ddagger}/\Delta G^{\ddagger}$ in kcal mol^{-1}) for Isomerization with Different η^1(C^3) Configurations of the Generic [(Octadienediyl)Ni^{II}PH$_3$] Complex as Precursors[a,b]

	TS$_{ISO}$[**3**]	TS$_{ISO}$[**3**-BD][c]	TS$_{ISO}$[**5**]	TS$_{ISO}$[**6**]
$\Delta H_{abs}^{\ddagger}/\Delta G_{abs}^{\ddagger}$[d]	13.0/*13.2*	12.6/*25.8*	24.9/*38.9*	21.8/*35.1*
$\Delta H_{int}^{\ddagger}/\Delta G_{int}^{\ddagger}$[e]	7.3/*8.2*	6.9/*8.0*	7.1/*8.2*	6.6/*7.0*

[a] The transition states are denoted according to the η^1(C^3)-precursors. [b] Numbers in italics are the Gibbs free energies. [c] The participation of butadiene is considered explicitly. [d] Absolute barriers relative to the most stable [(octadienediyl)Ni^{II}PH$_3$] species; namely, [(bis(η^3-syn)-octadienediyl)Ni^{II}PH$_3$] **4** + *trans*-BD. [e] Intrinsic barriers relative to the corresponding [(η^1(C^3)-octadienediyl)Ni^{II}PH$_3$] precursor.

Table 4. Activation Enthalpies and Free Energies ($\Delta H^{\ddagger}/\Delta G^{\ddagger}$ in kcal mol^{-1}) for Isomerization along the Most Feasible Pathway via TS$_{ISO}$[**3**] for the Generic [(Octadienediyl)Ni^{II}PH$_3$] Complex[a−c]

	η^3-syn,η^1(C^3)-syn → η^3-syn,η^1(C^3)-anti	η^3-anti,η^1(C^3)-syn → η^3-anti,η^1(C^3)-anti
$\Delta H_{abs}^{\ddagger}/\Delta G_{abs}^{\ddagger}$	13.0/*13.2* // 15.3/*15.3*	19.9/*19.8* // 22.1/*21.8*

[a] The isomerization barriers for SF and OF coupling species are separated by a double slash. [b] Absolute barriers relative to the most stable [(octadienediyl)Ni^{II}PH$_3$] species, namely, [(bis(η^3-syn)-octadienediyl)Ni^{II}PH$_3$] **4** + *trans*-BD. [c] Numbers in italics are the Gibbs free energies.

There are at least three different η^1(C^3) species conceivable as precursor structures for syn−anti isomerization, namely, the [(η^3,η^1(C^3)-octadienediyl)Ni^{II}L] species **3**, the [(η^1(C^1),η^1(C^3)-octadienediyl)Ni^{II}L] species **5**, and the [(bis(η^1(C^3))-octadienediyl)Ni^{II}L] species **6** (Scheme 1). We have located several isomers of the transition states for isomerization for each of these species. The energetically preferred transition states, which constitute the internal rotation of the vinyl group around the formal C^2−C^3 single bond, are shown in Figure S2 and the energetics is summarized in Table 3. For isomerization following the route starting from the formal 16e$^-$ species **3**, the influence of an additional coordinating butadiene on the activation barrier was explicitly examined.

In terms of absolute barriers, it is quite obvious from Table 3 that the most feasible route for isomerization starts from **3** and proceeds through TS$_{ISO}$[**3**]. The participation of butadiene in this process decreases the enthalpic barrier ($\Delta H^{\ddagger}$) by only 0.4 kcal mol^{-1} which, however, cannot compensate for the entropic cost of 12.6 kcal mol^{-1} caused by complexation of butadiene. Isomerizations via the bis(η^1) species **5** and **6** is less likely due to prohibitively high (essentially thermodynamic) absolute barriers. It is interesting to note, that the intrinsic barriers relative to the corresponding η^1(C^3) precursors **3**, **5**, and **6** ($\Delta G_{int}^{\ddagger}$ ∼7−8 kcal mol^{-1}, see Table 3) are very similar for all three competing isomerization routes.

The barriers for isomerization of the terminal allylic groups in the [(octadienediyl)Ni^{II}PH$_3$] complex along the preferred route via TS$_{ISO}$[**3**] are collected in Table 4. For isomerization involving η^3-syn,η^1(C^3) species, the barrier is ∼7 kcal mol^{-1} ($\Delta G^{\ddagger}$) lower than for the corresponding η^3-anti,η^1(C^3) species. These systems are linked together via a η^3-anti,η^1-syn → η^3-syn,η^1-anti conversion (and vice versa). Linear transit calculations reveal that no significant barrier is associated with this intramolecular $\eta^3/\eta^1 \rightarrow \eta^1/\eta^3$ shift. Overall the highest free-energy barrier for the isomerization amounts to 21.8 kcal mol^{-1} ($\Delta G^{\ddagger}$), which is lower than the barriers for the reductive elimination processes (section D) that complete the catalytic cycle.

C2. Isomerization of SF and OF Coupling Stereoisomers of the [(Octadienediyl)Ni^{II}L] Complex. As mentioned in

Table 5. Activation Enthalpies and Free Energies ($\Delta H^{\ddagger}/\Delta G^{\ddagger}$ in kcal mol^{-1}) and Reaction Enthalpies and Free Energies ($\Delta H/\Delta G$ in kcal mol^{-1}) for Reductive Elimination Affording VCH for the Generic [(Octadienediyl)Ni^{II}PH$_3$] Complex along **2** → **8** and **2** → **8′**[a−e]

BD coupling[a] isomer of **2**[a]	*t*/*t*-BD SF η^3-syn,Δ-t	*t*/*t*-BD OF η^3-syn,Δ-t	*c*/*t*-BD SF η^3-syn,Δ-c	*c*/*t*-BD OF η^3-syn,Δ-c	*c*/*c*-BD SF η^3-anti,Δ-c	*c*/*c*-BD OF η^3-anti,Δ-c
2	14.5/*13.5*	19.0/*18.0*	4.4/*4.1*	1.8/*1.5*	2.5/*2.3*	7.3/*7.2*
TS[**2**−**8**]			27.4/*27.4*	28.5/*28.5*	**25.0/*25.3***	30.9/*30.8*
8			−10.5/−*9.5*	−10.5/−*9.5*	−10.9/−*10.2*	−10.5/−*10.2*
2-BD	10.7/*23.0*	15.3/*27.2*	4.5/*17.3*	2.6/*15.4*	5.9/*18.4*	10.6/*23.5*
TS[**2**−**8′**]			20.0/*32.7*	**18.9/*31.9***	19.4/*32.7*	22.9/*36.0*
8′			−22.9/−*10.8*	−22.9/−*10.8*	−21.2/−*9.1*	−21.2/−*9.1*
5	38.7/*51.4*	39.5/*52.3*	20.4/*33.3*	17.8/*30.8*	17.9/*31.1*	20.1/*33.2*

[a] This process is classified according to the butadiene coupling stereoisomers involved. The relation between the butadiene coupling and the stereoisomers of **2** is explicitly given. [b] The thermodynamic stability of isomers of the bis-η^1 species **5** is added for comparison. [c] Absolute barriers relative to the most stable [(octadienediyl)Ni^{II}PH$_3$] species; namely, [(bis(η^3-syn)-octadienediyl)Ni^{II}PH$_3$] **4** + *trans*-BD. [d] Numbers in italics are the Gibbs free energies. [e] The lowest barrier of the individual stereochemical pathways is in boldface type.

section C1, allylic syn−anti isomerization is accompanied by an inversion of the allylic group's enantioface. Additionally, the interconversion of SF and OF butadiene coupling stereoisomers of the [(octadienediyl)Ni^{II}L] complex can take place by inverting the allylic group's enantioface without altering the allylic group's configuration, namely, anti or syn. This process preferably proceeds in the $\eta^3,\eta^1(C^1)$ species **2** by interconverting the σ-allylic group (Figure 2). The key species involved are given in Figure S3 for a representative case. The overall largest barrier of 14.3 kcal mol^{-1} ($\Delta G^{\ddagger}$) for interconversion in the η^3-syn,$\eta^1(C^1)$,Δ-cis isomer of **2** indicates the SF−OF isomerization as a facile process.

The kinetic results for both the syn−anti and SF−OF isomerization indicate that these processes are the most facile of all elementary reaction steps in the catalytic cycle, involving the [(octadienediyl)Ni^{II}L] complex. Accordingly, all the stereoisomers of the [(octadienediyl)Ni^{II}L] species **2**−**7** can be assumed to be in dynamic preequilibrium. Bis(η^1) species, however, are not involved in either of the isomerization processes along the most feasible pathway.

D. Formation of the Cyclodimer Products via Reductive Elimination under Ring Closure. In this section, we discuss the three competing reaction paths for reductive elimination from the [(octadienediyl)Ni^{II}L] species **2**−**4** to the [(cyclodimer)Ni^{0}L] products **8**−**10**. At least two distinct routes were explored for each of these paths, corresponding to the two mechanistic proposals for the reductive elimination process, where either η^3- or bis(η^1) species are assumed to be the direct precursors. Additionally, for the pathways starting from the formal 16e$^-$ species **2** and **3**, the participation of an additional butadiene was explicitly examined. The stereoisomers involved in the reductive elimination for each reaction path will be classified according to the kind of butadiene coupling to which the precursor corresponds. The relation between the butadiene coupling, the stereoisomers of the precursor, and (if required) the isomeric form of the cyclodimer product is explicitly reported (cf. Tables 5−7). Due to the preestablished equilibrium between all [(octadienediyl)Ni^{II}L] species, it is reasonable to operate with absolute barriers relative to the most stable species, which is the bis(η^3-syn) isomer of **4**.

D1. Formation of VCH. The formation of VCH proceeds along the branch commencing from the $\eta^3,\eta^1(C^1)$ species **2** via formation of a C−C σ-bond between the C^3 of the η^3-allylic moiety and the terminal C^8 of the η^1-allylic moiety (Figure S4). The reaction from the formal 16e$^-$ species **2** along the direct route, which does not involve the bis(η^1) species **5**, leads either to the [(η^4-VCH)Ni^{0}L] product **8** or to the [(η^2-VCH)(η^2-*trans*-butadiene)Ni^{0}L] product **8′** when an additional butadiene participates. For the alternative suggested **2** → **5** → **8′** route, butadiene has to take part since we found butadiene coordination was a prerequisite for the formation of the crucial bis(η^1) intermediate **5** (section B).

The formal 16e$^-$ product complex **8** is characterized by the coordination of both the vinyl group and the cyclohexene's double bond to nickel. Compound **8** is converted into the [(VCH)(butadiene)Ni^{0}L] complex **8′** via butadiene complexation. Similar to the findings for the active catalyst **1**, the most stable isomer of **8′** is a formal 16e$^-$ trigonal planar [(η^2-VCH)-(η^2-*trans*-butadiene)Ni^{0}PH$_3$] species, with VCH coordinating by its vinyl group to nickel. From **8′**, VCH is liberated via a subsequent substitution with butadiene which is exogonic by 4.4 kcal mol^{-1} (ΔG). The barrier associated with this process is supposed to be moderate and is expected to be significantly lower than that of the oxidative coupling and reductive elimination steps.

The key species for reductive elimination along **2** → **8** (without additional butadiene involved) and **2** → **8′** (with complexation of an additional butadiene) are shown in Figure S4 and the energetics for the different stereoisomers is collected in Table 5. Along **2** → **8**, the six-membered ring is generated by formation of a C−C σ-bond between C^3 and C^8 in the square-planar TS[**2**−**8**], which occurs at a distance of ∼2.0−2.1 Å of the newly formed bond (Figure S4). In the productlike TS[**2**−**8**], the η^3-allylic group is partly converted into a vinyl group and VCH is essentially formed. TS[**2**−**8**] leads to **8** by coordination of the cyclohexene's double bond to nickel. The **2** → **8′** route starts with the formal 18e$^-$ η^2-butadiene adduct of **2**, which is characterized by a trigonal bipyramidal coordination of the nickel center. We have located several isomers of this adduct. In the thermodynamically most stable isomers, the η^1-allylic moiety occupies an axial position and both the η^2-*trans*-butadiene and the ligand L reside at equatorial positions. The complexation of butadiene leads to a relaxation in the coordination sphere around nickel. Both allylic parts begin to move out of the coordination sphere of nickel during the reductive elimination. As a result, TS[**2**−**8′**] occurs earlier at a distance of ∼2.2 Å of the newly formed bond. TS[**2**−**8′**] decays into **8′**, which is accompanied by rotation of the coordinated vinyl group into a coplanar orientation with the η^2-butadiene.

For reductive elimination along the most feasible of the stereochemical pathways, the participation of butadiene lowers the enthalpic barrier ($\Delta H^{\ddagger}$) by 6.1 kcal mol^{-1} (Table 5). This,

Table 6. Activation Enthalpies and Free Energies ($\Delta H^{\ddagger}/\Delta G^{\ddagger}$ in kcal mol^{-1}) and Reaction Enthalpies and Free Energies ($\Delta H/\Delta G$ in kcal mol^{-1}) for Reductive Elimination Affording DVCB for the Generic [(Octadienediyl)Ni^{II}PH$_3$] Complex along **3** → **9**, **3** → **9′**, and **4** → **9**[a−e]

BD coupling[a] isomer of **4**[a] DVCB isomer[a]	*t*/*t*-BD SF bis(η^3-syn) trans-1,2	*t*/*t*-BD OF bis(η^3-syn) cis-1,2	*c*/*t*-BD SF η^3-anti/syn cis-1,2	*c*/*t*-BD OF η^3-anti/syn trans-1,2	*c*/*c*-BD SF bis(η^3-anti) trans-1,2	*c*/*c*-BD OF bis(η^3-anti) cis-1,2
3	5.7/*5.0*	7.2/*6.6*	13.6/*12.9*	13.0/*12.1*	14.0/*13.1*	14.0/*13.0*
TS[**3**−**9**]	**34.8**/***34.1***	35.5/*34.7*	38.8/*37.7*	36.6/*35.5*	35.9/*34.8*	41.6/*40.4*
9	13.8/*13.9*	3.0/*3.2*	7.9/*8.0*	16.2/*16.4*	18.0/*18.2*	19.4/*19.6*
3-BD	5.6/*17.8*	6.1/*18.4*	14.9/*26.8*	15.8/*27.8*	16.5/*28.9*	14.2/*26.7*
TS[**3**−**9′**]	**24.2**/***36.4***	27.2/*39.3*	29.7/*41.6*	25.6/*37.8*	25.0/*36.9*	29.9/*42.2*
9′	−1.9/*9.4*	2.7/*14.1*	2.7/*14.1*	−1.9/*9.4*	−1.9/*9.4*	2.7/*14.1*
4	6.5/*6.8*	0.0/*0.0*	2.4/*2.8*	8.4/*8.8*	3.1/*2.8*	8.2/*7.7*
TS[**4**−**9**]	33.4/*33.7*	28.0/*28.4*	**22.3**/***22.7***	31.4/*32.1*	40.7/*41.0*	23.5/*23.8*
9	13.8/*13.9*	3.0/*3.2*	7.9/*8.0*	16.2/*16.4*	18.0/*18.2*	2.1/*2.3*
6	15.7/*28.4*	16.3/*29.4*	17.2/*30.0*	15.2/*28.1*	15.7/*28.0*	17.9/*30.8*

[a] This process is classified according to the butadiene coupling stereoisomers involved. The relation between the butadiene coupling, the stereoisomers of **4**, and the DVCB stereoisomers formed is explicitly given. [b] The thermodynamic stability of isomers of the bis-η^1 species **6** is added for comparison. [c] Absolute barriers relative to the most stable [(octadienediyl)Ni^{II}PH$_3$] species, namely, [(bis(η^3-syn)-octadienediyl)Ni^{II}PH$_3$] **4** + *trans*-BD. [d] Numbers in italics are the Gibbs free energies. [e] The lowest barrier of the individual stereochemical pathways is in boldface type.

however, cannot compensate the decrease in entropy associated with butadiene complexation, which amounts to 13 kcal mol^{-1}. Therefore, the reductive elimination affording VCH along a direct **2** → **8** route is less likely to be assisted by coordination of an additional butadiene. A free-energy barrier of 25.3 kcal mol^{-1} ($\Delta G^{\ddagger}$) has to be overcome for the most feasible pathway along **2** → **8**. It should be noted, that VCH cannot be formed from the η^3-syn,η^1(C^1),Δ-trans isomers of **2** that originate from a *trans*/*trans*-butadiene coupling. At first these isomers have to undergo isomerization in order to generate a six-membered ring containing a cis double bond.

Following the alternative mechanistic proposal, the bis(η^1) species **5** is postulated as intermediate along the reaction path affording VCH. We have located several isomers of **5**, the square-pyramidal species with a η^4-*cis*-butadiene coordinated is the most stable (Figure 3). We should note here again that bis(η^1) species generally are of high energy; in fact, **5** is energetically very similar to TS[**2**−**8′**] (Table 5). Following the reaction pathway in a linear transit approach[28] starting from different isomers of **5** reveals a facile η^1(C^3) → η^3 allylic rearrangement which always leads to the same type of transition states as for the **2** → **8′** route. The transition state connected with **5**, which we have not been able to locate, however, is expected to be energetically very high and well separated from TS[**2**−**8′**]. This let us to conclude that the bis(η^1) species **5** is precluded from the energetically most favorable route. The formation of VCH preferably take place along the direct **2** → **8** path.

D2. Formation of DVCB. Two different [(octadienediyl)-Ni^{II}L] species are conceivable as precursors in the formation of DVCB, namely, **3** and **4**. Starting from the formal 16e$^-$ η^3,η^1-(C^3) species **3**, either the [(η^4-DVCB)Ni^{0}L] product **9** or the [(DVCB)(butadiene)Ni^{0}L] complex **9′** is formed depending on whether butadiene is involved (**3** → **9′**) or not involved (**3** → **9**). However, butadiene is less likely to participate for the direct **4** → **9** route when starting from the formal 18e$^-$ species **4** that leads to **9**. For the alternative proposed route involving the postulated bis(η^1) species **6**, namely, **4** → **6** → **9′**, butadiene coordination is critical for stabilizing **6**. The most stable isomer of **9′** is a formal 16e$^-$ trigonal planer [(η^2-DVCB)(η^2-*trans*-butadiene)Ni^{0}PH$_3$] species. The product **9**, which is formed along the direct routes from **3** or **4** without involving butadiene (**3** → **9**, **4** → **9**), is converted into **9′** via butadiene complexation. DVCB is expelled through a subsequent exothermic substitution with butadiene ($\Delta G = -5.1$ kcal mol^{-1}), which regenerates the active catalyst **1**.

The key species along **3** → **9** and **3** → **9′** (Figure S5) resemble those for the VCH formation via the **2** → **8** and **2** → **8′** pathways (Figure S4) very closely, except that a four-membered ring is generated for production of DVCB by forming a C−C σ-bond between C^3 and C^6, while for production of VCH, a six-membered ring is formed by closing the bond between C^3 and C^8. On the other hand, DVCB can be generated along **4** → **9** by establishing a σ-bond between the substituted terminal carbons (C^3, C^6) of two η^3-allylic groups in the formal 18e$^-$ square-pyramidal bis(η^3) species **4** (Figure S5). The transition state TS[**4**−**9**] occurs at a distance of ∼1.9 Å for the newly formed bond and is characterized by a partly η^3-allyl → vinyl conversion of both allylic groups and decays into **9** where DVCB is coordinated to Ni^0 by its two vinyl groups.

To examine the **4** → **6** → **9′** route, we have first located several isomers of the critical intermediate **6**. The most stable one is the square-pyramidal η^4-*cis*-butadiene coordinated species that is energetically well separated from **3** and **4** by more than 24 kcal mol^{-1} (ΔG) (Figure 3). While trying to locate transition states in a linear transit approach[28] starting from **6**, we found again (see section D1) a facile η^1(C^3) → η^3 conversion of one allylic group leading to the TS[**3**−**9′**] transition state. Although we have not located the transition state that is directly connected with **6**, we expect it to be significantly higher in energy than TS[**3**−**9′**]. We have to conclude that there is no viable route with the bis(η^1) species **6** involved. DVCB is most probably formed along the direct reductive elimination route starting from the [(η^3-octadienediyl)Ni^{II}L] precursors **3** or **4** and proceeding along either **3** → **9**, **3** → **9′**, or **4** → **9**.

The energetics for these routes are collected in Table 6 for different stereochemical pathways. Similar to the findings for VCH formation (**2** → **8**, section D1), butadiene is less likely to participate along the direct route starting from **3** that does not involve the bis(η^1) species **6**. The comparison of the barriers for the most feasible of the stereochemical pathways for **3** → **9** and **4** → **9** reveals the kinetic preference of the **4** → **9** route,

(28) In the linear transit approach, the distance of the two carbons of the newly formed bond is chosen as the reaction coordinate.

Table 7. Activation Enthalpies and Free Energies ($\Delta H^{\ddagger}/\Delta G^{\ddagger}$ in kcal mol^{-1}) and Reaction Enthalpies and Free Energies ($\Delta H/\Delta G$ in kcal mol^{-1}) for Reductive Elimination Affording COD for the Generic [(Octadienediyl)Ni^{II}PH$_3$] Complex along **4** → **10** and **4** → **7** → **10′**[a–d]

BD coupling[a] isomer of **4**[a] COD isomer[a]	*t*/*t*-BD SF bis(η^3-syn) trans,trans	*t*/*t*-BD OF bis(η^3-syn) trans,trans	*c*/*t*-BD SF η^3-anti/syn cis,trans	*c*/*t*-BD OF η^3-anti/syn cis,trans	*c*/*c*-BD SF bis(η^3-anti) cis,cis	*c*/*c*-BD OF bis(η^3-anti) cis,cis
4	6.5/*6.8*	0.0/*0.0*	2.4/*2.8*	8.4/*8.8*	3.1/*2.8*	8.2/*7.7*
TS[**4**−**10**]	58.2/*59.5*	61.8/*62.1*	40.7/*41.7*	43.7/*45.1*		**21.6**/***22.5***
10	53.5/*54.0*	60.3/*60.9*	29.3/*29.7*	29.3/*29.7*		−0.7/*−0.2*
7[29]						18.3/*29.3*
TS[**7**−**10′**][29]						**23.2**/***35.4***
10′[29]						13.8/*−1.5*

[a] This process is classified according to the butadiene coupling stereoisomers involved. The relation between the butadiene coupling, the stereoisomers of **4**, and the COD stereoisomers formed is explicitly given. [b] Absolute barriers relative to the most stable [(octadienediyl)Ni^{II}PH$_3$] species; namely, [(bis(η^3-*syn*)-octadienediyl)Ni^{II}PH$_3$] **4** + *trans*-BD. [c] Numbers in italics are the Gibbs free energies. [d] The lowest barrier of the individual stereochemical pathways is in boldface type.

which is favored by ∼11 kcal mol^{-1} ($\Delta G^{\ddagger}$) over **3** → **9**. We conclude that reductive elimination leading to DVCB preferably takes place starting from the bis(η^3) precursor **4** along the direct path **4** → **9**. We shall focus on this path in the further discussion about the stereocontrol of the DVCB formation.

The calculated barriers for different stereochemical pathways along **4** → **9** reflect a notable trend. The reductive elimination barrier is significantly lower for pathways involving stereoisomers of **4** that originate from a OF coupling of two *cis*- or *trans*-butadienes or from a *cis*/*trans*-butadiene SF coupling, when compared to the opposite coupling stereoisomers (Table 6). DVCB exists in two isomeric forms, namely, cis-1,2 and trans-1,2, which relates to the position of the two vinyl groups on the four-membered ring. For free DVCB, the trans-1,2 isomer is 2.4 kcal mol^{-1} (ΔG) more stable than the cis-1,2 isomer. Reductive elimination with *cis*/*cis*- and *trans*/*trans*-butadiene OF coupling and *cis*/*trans*-butadiene SF coupling stereoisomers leads to the kinetically preferred *cis*-1,2-DVCB with a barrier of 22.7 kcal mol^{-1} ($\Delta G^{\ddagger}$) for the most feasible pathway, while formation of *trans*-1,2-DVCB is kinetically hindered by a barrier that is more than 9 kcal mol^{-1} ($\Delta G^{\ddagger}$) higher (Table 6). That agrees with the experimental observation of only the cis-1,2 isomer of DVCB in the reaction product.[11] From the barriers for the individual stereochemical pathways for oxidative coupling and reductive elimination affording *cis*-1,2-DVCB, it is quite obvious that these two steps operate under different stereocontrol since opposite stereoisomers are involved along the most feasible of the pathways for each of these steps.

Overall, the [(η^4-DVCB)Ni^{0}PH$_3$] product **9** is generated in an endothermic process, with the reverse process, the oxidative addition under C−C bond cleavage, **9** → **4** has a significant lower barrier. The mechanistic implications will be discussed further in section E.

D3. Formation of COD. The bis(η^3) species **4** is the precursor for reductive elimination along the two competing reaction paths affording DVCB and COD. The generation of COD involves the formation of an eight-membered ring by establishing a C−C σ-bond between the terminal unsubstituted carbons (C^1, C^8) of the two η^3-allylic groups (Figure S6). Butadiene is found not to be involved in the direct process **4** → **10**, while the route **4** → **7** → **10′** involving the bis(η^1) species **7** requires butadiene participation. However, the [(η^4-COD)Ni^0-PH$_3$] complex **10** can coordinate butadiene affording the [(η^2-COD)(η^2-*trans*-butadiene)Ni^{0}PH$_3$] complex **10′**. From **10′**, the active catalyst **1** is regenerated under liberation of COD in an exothermic substitution with butadiene ($\Delta G = -4.6$ kcal mol^{-1}).

Transition-state structures have been located for both the process **4** → **10** and the **4** → **7** → **10′** route.[29] In contrast to the bis(η^1) species **5** and **6**, there is no facile pathway for a η^1(C^1) → η^3 allylic rearrangement in **7**. The key structures along the two routes leading to *cis*,*cis*-COD are displayed in Figure S6 and the energetics is summarized in Table 7. Along the direct **4** → **10** route, TS[**4**−**10**] occurs at a distance of ∼2.1 Å for the newly formed C−C σ-bond and decays into the [(η^4-COD)Ni^0-PH$_3$] product **10**. Concerning the *cis*/*cis*-butadiene SF coupling bis(η^3-anti) stereoisomer of **4**, the corresponding transition state TS[**4**−**10**] could not be located, since C−C bond formation between the two trans-oriented terminal η^3-allyl carbons (C^1, C^8) affords a highly strained transition-state structure. Several isomers have been located for the bis(η^1) intermediate **7** of the alternative process **4** → **7** → **10′**. The most stable isomer (at the ΔG surface) has a coordinated η^2-*trans*-butadiene, although isomeric forms with either a η^2-trans or a η^4-cis coordinated butadiene are very similar in enthalpy. The most favorable isomer of TS[**7**−**10′**] is characterized by a η^2-*trans*-butadiene coordination and occurs at a distance of ∼2.1 Å for the newly formed C−C bond. For the η^4-cis isomers of **7**, the butadiene always undergoes a η^4 → η^2 rearrangement in the vicinity of the transition state.

The calculated barriers for different stereochemical pathways along **4** → **10** are largely affected by steric strain. The reductive elimination with the OF coupling bis(η^3-anti) stereoisomer of **4** has the lowest free-energy barrier of 22.5 kcal mol^{-1} ($\Delta G^{\ddagger}$). This gives rise to the thermodynamically most stable *cis*,*cis*-COD isomer, which is formed in an overall thermoneutral reaction. However, the formation of *trans*,*trans*-COD from the OF coupling bis(η^3-syn) stereoisomer of **4** has an insurmountable high barrier of 62.1 kcal mol^{-1} ($\Delta G^{\ddagger}$). This leads to the highly strained *trans*,*trans*-COD product isomer **10**, which is only 1.2 kcal mol^{-1} (ΔG) below the transition state and by 61.1 kcal mol^{-1} (ΔG) less stable than the *cis*,*cis*-COD isomer of **10**.

Comparison of the barriers associated for the two proposed routes for *cis*,*cis*-COD generation (Table 7) demonstrates that the direct process **4** → **10** is favored over **4** → **7** → **10′**, by 12.9 kcal mol^{-1} in terms of free energy ($\Delta\Delta G^{\ddagger}$) and by 1.6 kcal mol^{-1} in terms of enthalpy ($\Delta\Delta H^{\ddagger}$). For the process **4** → **10**, *cis*,*cis*-COD is the kinetically and thermodynamically preferred product, and the formation of the other isomers, in particular *trans*,*trans*-COD, is precluded by distinct higher kinetic barriers due to steric strain. That agrees with the experimental observa-

(29) We focused only on the most viable formation of *cis*, *cis*-COD along **4** → **7** → **10′**.

tion that *cis*,*cis*-COD is the only isomer of COD that is formed in the [Ni^{0}L]-catalyzed cyclodimerization of butadiene.[11]

E. Regulation of the Selectivity of the Cyclodimer Formation. The structural and energetic characterization of all critical elementary steps of the entire catalytic cycle allows us to address how the selectivity of the cyclodimer formation is controlled. We are here just outlining the principles derived from the present investigation of the generic [bis(butadiene)Ni^{0}PH$_3$] catalyst. A comprehensive and detailed analysis of how the electronic and steric properties of the ligand L affect the regulation of the product selectivity is presented in a forthcoming study.

E1. Thermodynamic Regulation of the Product Selectivity. The [(octadienediyl)Ni^{II}L] complex represents the crucial compound for the entire catalytic cycle. The $\eta^3,\eta^1(C^1)$ species **2** is the precursor for reductive elimination to give VCH, and the bis(η^3) species **4** is the starting point for the two reaction paths that yield *cis*-1,2-DVCB and *cis*,*cis*-COD. The different conformations are in equilibrium, and the conversion between the individual stereoisomers by syn−anti and SF−OF isomerization of the terminal allylic groups in the η^3,η^1 species **3** and **2**, respectively is predicted to be the most facile elementary process involving the [(octadienediyl)Ni^{II}L] complex. For that reason, all [(octadienediyl)Ni^{II}L] species are in a kinetically mobile preestablished equilibrium that can be regarded as always being attained. This let us to conclude that the selectivity of the cyclodimer production is regulated thermodynamically by the position of this preestablished equilibrium, which determines the thermodynamic populations of **2** and **4**. For the generic [bis(butadiene)Ni^{0}PH$_3$] catalyst examined in the present study, **2** and **4** are predicted to have similar populations (see section B). The equilibrium, however, is shown to be strongly influenced by the electronic and steric properties of the ligand L.[11,12] Experiment demonstrated that the equilibrium is shifted entirely to **2** for bulky, basic phosphines.[13] Therefore, VCH should be formed as the predominant cyclodimer for these ligands L,[30] since the *cis*,*cis*-COD and *cis*-1,2-DVCB generating reaction paths are precluded thermodynamically by the negligibly concentration of **4**. On the other hand, the paths for production of *cis*,*cis*-COD and *cis*-1,2-DVCB will be available under thermodynamic control for less basic ligands L, since in that case the formation of **4** is favored.[13]

E2. Kinetic Regulation of the Product Selectivity. The reductive elimination steps have the highest barriers in the catalytic cycle and are, therefore, predicted to be rate-determining. Since the precursor species **2** and **4** are in mobile preestablished equilibrium, the difference in the absolute reductive elimination barriers ($\Delta\Delta G^{\ddagger}$) for the three reaction paths regulates kinetically the selectivity of cyclodimer formation. Concerning the generic [bis(butadiene)Ni^{0}PH$_3$] catalyst, nearly identical free-energy barriers have to be overcome for production of *cis*-1,2-DVCB and *cis*,*cis*-COD along the most feasible pathways for **4** → **9** and **4** → **10** (Table 8). The formation of VCH, however, is kinetically impeded by a higher barrier of 2.8 kcal mol^{-1} ($\Delta\Delta G^{\ddagger}$). This would suggest that *cis*,*cis*-COD and *cis*-1,2-DVCB should be formed in a 50−50% mixture by the generic [bis(butadiene)Ni^{0}PH$_3$] catalyst. The reverse oxidative addition under C−C bond cleavage, however, also has to be taken into account for deciding which of the two cyclodimers is predominantly formed. The *cis*-1,2-DVCB product complex **9** and free *cis*-1,2-DVCB are significantly less stable than the *cis*,*cis*-COD product complex **10** and free *cis*,*cis*-COD, respectively (Tables 6 and 7). This would indicate that *cis*,*cis*-COD should be formed as the principal cyclodimer product, since the thermodynamically instable *cis*-1,2-DVCB would be rearranged under thermodynamic control into *cis*,*cis*-COD along **9** → **4** → **10**.

Table 8. Activation Enthalpies and Free Energies ($\Delta H^{\ddagger}/\Delta G^{\ddagger}$ in kcal mol^{-1}) for Reductive Elimination Affording VCH, *cis*-1,2-DVCB, and *cis*,*cis*-COD for the Generic [(Octadienediyl)Ni^{II}PH$_3$] Complex along the Most Feasible Stereochemical Pathway of the **2** → **8**, **4** → **9**, and **4** → **10** Routes, Respectively[a,b]

VCH η^3-anti,$\eta^1(C^1)$,Δ-cis SF **2** → **8**	*cis*–1,2-DVCB η^3-syn/η^3-anti SF **4** → **9**	*cis*,*cis*-COD bis(η^3-anti) OF **4** → **10**
25.0/*25.3*	22.3/*22.7*	21.6/*22.5*

[a] Absolute barriers relative to the most stable [(octadienediyl)Ni^{II}PH$_3$] species, namely, [(bis(η^3-syn)-octadienediyl)Ni^{II}PH$_3$] **4**. [b] Numbers in italics are the Gibbs free energies.

Our conclusions agree with the observed product distribution for a catalyst with a less basic PR$_3$ or P(OR)$_3$ ligand L.[31] For these catalysts, *cis*-1,2-DVCB can be isolated in up to 40% yield together with *cis*,*cis*-COD by carrying out the cyclodimerization reaction under mild conditions (40−50 °C) and if the reaction is terminated before complete conversion of the butadiene has occurred (<85%), while formation of VCH is essentially suppressed.[7,11,18] After complete conversion of butadiene, *cis*-1,2-DVCB is rearranged into *cis*,*cis*-COD, which is then formed quantitatively (over 96% selectivity) after a certain period as the thermodynamically more stable cyclodimer.[18]

Concluding Remarks

We have presented a comprehensive theoretical study of the mechanism for the [Ni^{0}L]-catalyzed cyclodimerization of butadiene employing a gradient-corrected DFT method. We have explored the important elementary reactions of the whole catalytic cycle for the generic [bis(butadiene)Ni^{0}PH$_3$] catalyst, namely, oxidative coupling of two butadienes, reductive elimination under ring closure, and allylic syn−anti and enantioface (SF−OF) conversion. The different species and stereoisomers of the crucial [(octadienediyl)Ni^{II}PH$_3$] complex have been studied in detail. The key species of individual stereochemical pathways along different routes have been structurally and energetically characterized. Based on this work, we present here a condensed mechanistic scheme for the entire catalytic cycle consisting of the most feasible routes for the important elementary reaction processes (Scheme 2).

Oxidative coupling of the two butadienes in **1** to give **2** as the kinetic coupling product preferably takes place via formation of a C−C σ-bond between the outermost carbons of two η^2-butadiene moieties. The lowest barrier arises from the *cis*/*trans*-butadiene coupling, which also leads to the thermodynamically most stable isomer of **2** in a thermoneutral process. The coupling

(30) VCH would not be formed quantitatively, since the generation of cyclotrimer products along an alternative route has to be taken into account. We are here concerned with the [Ni^{0}L]-catalyzed cyclodimerization of butadiene and the theoretical exploration of the Ni^0-catalyzed cyclotrimerization of butadiene will be reported elsewhere.

(31) Although PH$_3$ does not represent properly the electronic properties of either phosphines or phosphites, it is reasonabe to assume that PH$_3$ could serve as a model for a less basic ligand L rather than for a strong basic ligand.

Scheme 2. Condensed Gibbs Free-Energy Profile (kcal mol^{-1}) of the Entire Catalytic Cycle of the [Ni^{0}L]-Catalyzed Cyclodimerization of Butadiene by the Generic [Bis(butadiene)Ni^{0}PH$_3$] Catalyst

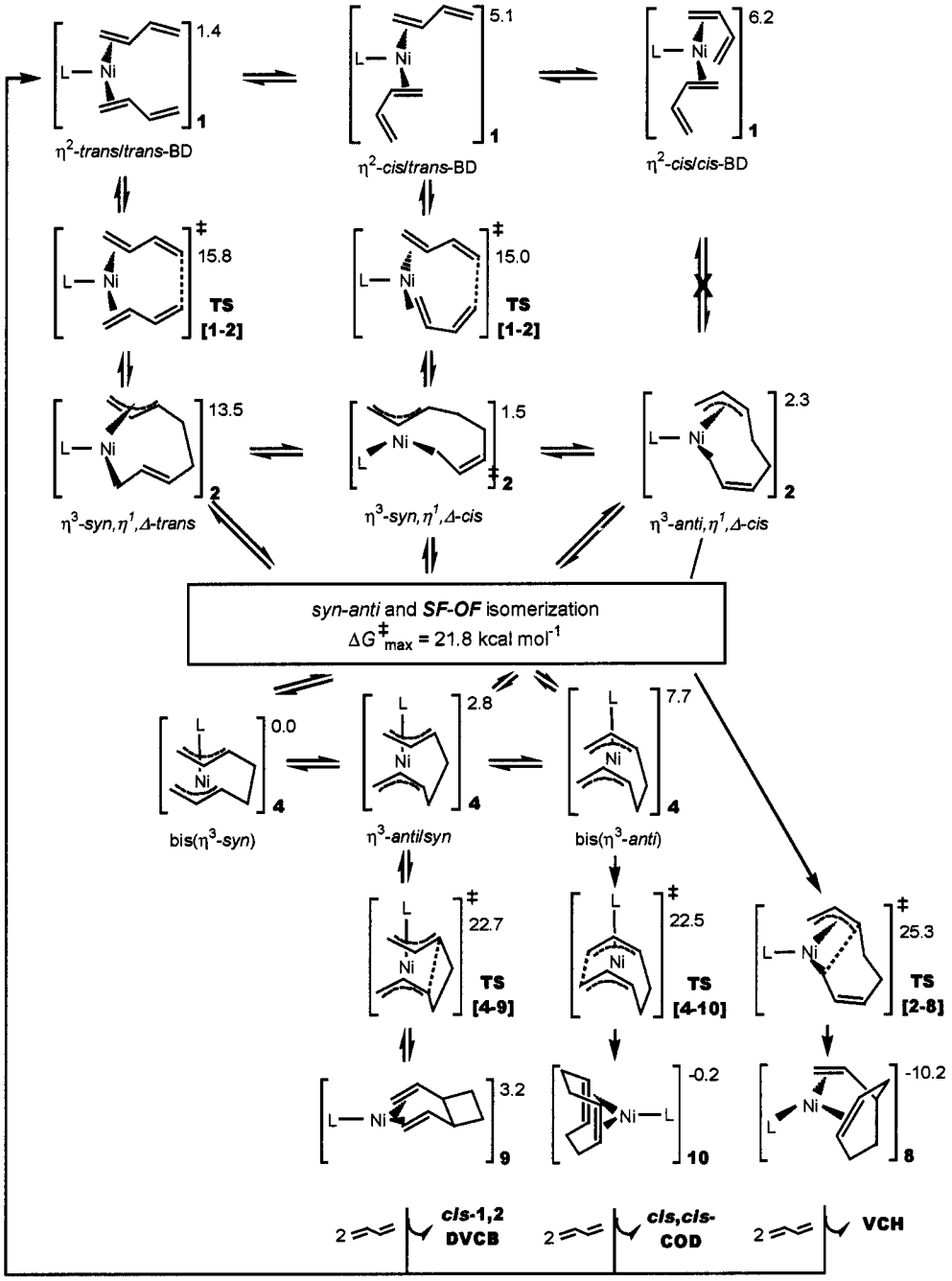

of two *trans*-butadienes is accompanied by a slightly higher barrier, while the coupling of two *cis*-butadienes must be considered as kinetically less likely.

The [(octadienediyl)Ni^{II}L] complex is the crucial compound of the catalytic cycle. Among the several possible configurations of this complex, all of which are in equilibrium, the $\eta^3,\eta^1(C^1)$ species **2** and the bis(η^3) species **4** are found to be thermodynamically most stable. They are predicted to be present in equal amounts for the generic catalyst (L = PH$_3$).

The present study indicates that bis(η^1) species play no role as intermediates in the catalytic cycle either in reductive elimination or in isomerization.

Syn−anti isomerization most likely takes place in the η^3,η^1-(C^3) species **3**, and the interconversion of SF and OF stereoisomers preferably proceeds in the $\eta^3,\eta^1(C^1)$ species **2**. The different [(octadienediyl)Ni^{II}L] species and their stereoisomers can be assumed to be in dynamic preestablished equilibrium through the facile syn−anti and SF−OF isomerization processes prior to reductive elimination.

The formation of the cyclodimer products occurs via reductive elimination along three competing reaction paths. VCH is formed directly from **2** along **2** → **8,** and **4** is the precursor for both the formation of *cis*-1,2-DVCB along **4** → **9** and the **4** → **10** *cis,cis*-COD production path. From the [(cyclodimer)Ni^{0}L] products **8**−**10**, the cyclodimers are liberated in a subsequent exothermic substitution with butadiene, which regenerates the active catalyst **1**. We predict reductive elimination to be the rate-determining step in the catalytic cycle.

Oxidative coupling (in **1**) and reductive elimination (in **4**) operate under different stereocontrol since opposite butadiene coupling stereoisomers are involved along the most feasible of the pathways for these steps. The thermodynamic less stable *cis*-1,2-DVCB is the kinetically preferred product along **4** → **9**, while the generation of the *trans*-1,2-DVCB is kinetically less likely. *cis*,*cis*-COD is primarily generated along **4** → **10**, whereas the formation of other isomers, in particular *trans*,*trans*-COD, is precluded by distinctly higher kinetic barriers that originate from steric strain. Our results are in agreement with experimental observation and rationalize the exclusive production of the *cis*-1,2-DVCB and *cis*,*cis*-COD cyclodimers.

Concerning the generic [bis(butadiene)Ni^{0}PH$_3$] catalyst, similar barriers have to be overcome along the most feasible pathways for **4** → **9** and **4** → **10**, whereas the formation of VCH is kinetically impeded by a higher barrier. Nevertheless, *cis*,*cis*-COD is predicted to be formed as the principal cyclodimer product, since the thermodynamic instable *cis*-1,2-DVCB is rearranged via the reverse oxidative addition under C−C bond cleavage into the more stable *cis*,*cis*-COD along **9** → **4** → **10**. This closely parallels the experimental observation for catalysts with L = P(OR)$_3$, since PH$_3$ could be considered to model a less basic ligand L.

Acknowledgment. S.T. is grateful to Prof. Dr. Rudolf Taube for his ongoing interest in this research, which was a continual stimulation. S.T. is furthermore indebted to Prof. Dr. R. Ahlrichs (University of Karlsruhe, Germany) for making the latest version of TURBOMOLE available. Excellent service by the computer centers URZ Halle and URZ Magdeburg is gratefully acknowledged.

Supporting Information Available: Full descriptions of the geometries and energies of all species. Also included is the pictorial representation of key species involved in the important elementary steps along the most feasible pathway (Figures S1−S6) (PDF). This material is available free of charge via the Internet at http://pubs.acs.org.

JA012372T